Z-peak subtracted representation of Bhabha scattering and search for new physics effects

M. Beccaria[1,2] F. M. Renard,[3] S. Spagnolo,[4] and C. Verzegnassi[5,6]
[1]*Dipartimento di Fisica, Università di Lecce, Via Arnesano, 73100 Lecce, Italy*
[2]*INFN, Sezione di Lecce, Via Arnesano, 73100 Lecce, Italy*
[3]*Physique Mathématique et Théorique, UMR 5825, Université Montpellier II, F-34095 Montpellier Cedex 5, France*
[4]*Rutherford Appleton Laboratory–Particle Physics Department, Chilton, Didcot, Oxfordshire OX11 0QX, United Kingdom*
[5]*Dipartimento di Fisica Teorica, Università di Trieste, Strada Costiera 14, Miramare (Trieste), Italy*
[6] *INFN, Sezione di Trieste, Italy*
(Received 9 February 2000; published 24 July 2000)

To the special case of Bhabha scattering we extend the ''Z-peak subtracted'' representation previously applied to $e^+e^-\to f\bar{f}$ $(f\neq e)$. This allows us to analyze the process at any energy, while imposing in an automatic way the constraints set by high-precision measurements at the Z peak. The procedure turns out to be particularly convenient in a search for a certain class of new physics effects at variable energy. A few examples are considered, and the information thus obtained is combined with the corresponding information that can be derived from the other e^+e^- annihilation processes, both at present (CERN LEP2) and at future colliders. This shows that the role of Bhabha scattering in this respect can be quite relevant.

PACS number(s): 12.15.−y, 12.60.−i, 13.10.+q

I. INTRODUCTION

A convenient way of searching for virtual new physics effects in e^+e^- annihilation processes was recently proposed; it consists of the use of the so-called ''Z-peak subtracted representation'' that allows one to take into account automatically the severe constraints imposed by the high-precision measurements performed at the Z peak by the CERN e^+e^- collider LEP1 and SLAC Linear Collider [1]. This is achieved by choosing as ''theoretical input'' the measured values of the partial Z widths Γ_f and of the effective weak angle $\sin^2\theta_{\rm eff}$ together with $\alpha(0)$. For each $e^+e^-\to f\bar{f}$ $(f\neq e)$ annihilation process, all the one-loop standard model (SM) or new physics (NP) effects are described by four functions of the energy ($\sqrt{q^2}$) and of the scattering angle θ which are subtracted at $q^2=M_Z^2$ or at $q^2=0$ in order to take the inputs into account. We defer to Ref. [2] for further details.

This procedure is especially suitable for the search of NP effects which grow with the energy. Various applications were made for supersymmetry, technicolor, anomalous gauge couplings, higher Z' bosons, four-fermion contact terms and extra dimensions [2–6]. The description was shown [6] to be particularly useful when the NP is characterized by an effective scale Λ which is much higher than the actual energy range of $\sqrt{q^2}$. In the particular case of *universal* θ-independent effects, all the information on NP can be then conveyed into three constants called $\delta_{Z,s,\gamma}$, that can be viewed as the generalization, beyond the Z peak, of the T, S [7], or $\epsilon_{1,3}$ [8] descriptions.

This representation was not yet applied to Bhabha scattering because of the complication generated by the presence of t-channel photon and Z exchanges. The purpose of the present paper is to fill this lack. In Sec. II the whole Z-peak subtracted formalism can be extended to Bhabha scattering in a very natural way. This will allow one to use this process, together with the other $e^+e^-\to f\bar{f}$ processes, in order to improve the constraints on possible NP contributions, as illustrated in Sec. III. In Sec. IV, we shall show in numerical applications that the gain thus obtained can be substantial.

II. Z-PEAK SUBTRACTED REPRESENTATION

We shall first summarize the results of the Z-peak subtracted representation, described in previous papers [2], by writing the general $e^+e^-\to f\bar{f}$ $(f\neq e)$ scattering amplitude at one loop as the sum of an effective photon and an effective Z amplitude with couplings $g^{\gamma}_{Vj}(q^2,\theta)$, $g^{Z}_{Vj}(q^2,\theta)$, $g^{Z}_{Aj}(q^2,\theta)$, where the index j denotes either the initial electron ($j=e$) or the final fermion ($j=f\neq e$):

$$\begin{aligned}\mathcal{A}(q^2,\theta)=&\frac{i}{q^2}\bar{v}(e^+)\gamma^\mu g^{(\gamma)}_{Ve}(q^2,\theta)u(e^-)\\&\cdot\bar{u}(f)\gamma_\mu g^{(\gamma)}_{Vf}(q^2,\theta)v(\bar{f})\\&+\frac{i}{q^2-M_Z^2+iM_Z\Gamma_Z}\bar{v}(e^+)\gamma^\mu[g^{(Z)}_{Ve}(q^2,\theta)\\&-g^{(Z)}_{Ae}(q^2,\theta)\gamma^5]u(e^-)\cdot\bar{u}(f)\gamma_\mu[g^{(Z)}_{Vf}(q^2,\theta)\\&-g^{(Z)}_{Af}(q^2,\theta)\gamma^5]v(\bar{f}).\end{aligned}\tag{2.1}$$

The aforementioned inputs are taken into account by imposing that the total amplitude takes the required value at $q^2=0$ and at $q^2=M_Z^2$. Following the method of Ref. [2], this amounts to using a subtraction procedure which allows one to write

$$g_{Ve}^{\gamma}(q^2,\theta)=\sqrt{4\pi\alpha(0)}Q_e\left[1+\frac{1}{2}\tilde{\Delta}_{\alpha,ef}(q^2,\theta)\right],$$

$$g_{Vf}^{\gamma}(q^2,\theta)=\sqrt{4\pi\alpha(0)}Q_f\left[1+\frac{1}{2}\tilde{\Delta}_{\alpha,ef}(q^2,\theta)\right],$$

$$g_{Ae}^{\gamma}(q^2,\theta)=g_{Af}^{\gamma}(q^2,\theta)=0,$$

$$g_{Ve}^{Z}=\gamma_e^{1/2}I_{3e}\tilde{v}_e\left[1-\frac{1}{2}R_{ef}(q^2,\theta)-\frac{4\tilde{s}_e\tilde{c}_e}{\tilde{v}_e}|Q_f|V_{ef}^{\gamma Z}(q^2,\theta)\right],$$

$$g_{Vf}^{Z}(q^2,\theta)=\gamma_f^{1/2}I_{3f}\tilde{v}_f\left[1-\frac{1}{2}R_{ef}(q^2,\theta)-\frac{4\tilde{s}_e\tilde{c}_e}{\tilde{v}_f}|Q_f|V_{ef}^{Z\gamma}(q^2,\theta)\right],$$

$$g_{Ae}^{Z}(q^2,\theta)=\gamma_e^{1/2}I_{3e}\left[1-\frac{1}{2}R_{ef}(q^2,\theta)\right],$$

$$g_{Af}^{Z}(q^2,\theta)=\gamma_f^{1/2}I_{3f}\left[1-\frac{1}{2}R_{ef}(q^2,\theta)\right], \tag{2.2}$$

with the Z-peak inputs

$$\gamma_j^{1/2}=\left[\frac{48\pi\Gamma_j}{N_jM_Z(1+\tilde{v}_j^2)}\right]^{1/2} \tag{2.3}$$

and

$$\tilde{v}_j=1-4|Q_j|\tilde{s}_j^2, \tag{2.4}$$

where $\tilde{s}_j^2=1-\tilde{c}_j^2$ is the weak effective angle measured through the forward-backward or polarization asymmetries in the final channel j, $\tilde{s}_e\equiv\tilde{s}_\mu\equiv\tilde{s}_\tau$ and N_j is the color factor with QCD corrections at the Z peak.

The quantities $\tilde{\Delta}_{\alpha,ef}(q^2,\theta)$, $R_{ef}(q^2,\theta)$, $V_{ef}^{\gamma Z}(q^2,\theta)$, and $V_{ef}^{Z\gamma}(q^2,\theta)$ contain all the q^2- and θ-dependent parts of the scattering amplitude due to the SM or NP at one-loop. In our approach, they consist of certain finite combinations of self-energies, vertices, and boxes that are *automatically* gauge independent.

For an additional four-fermion amplitude,

$$\overline{v}(e^+)\gamma^\mu[a(q^2,\theta)-b(q^2,\theta)\gamma^5]u(e^-)\cdot\overline{u}(f)\gamma_\mu[c(q^2,\theta)-d(q^2,\theta)\gamma^5]v(f), \tag{2.5}$$

where a, b, c, and d are $\mathcal{O}(\alpha)$ quantities, one easily obtains the corresponding projections on the photon and Z Lorentz structures:

$$\tilde{\Delta}_{\alpha,ef}(q^2,\theta)=q^2\frac{[a(q^2,\theta)-b(q^2,\theta)\tilde{v}_e][c(q^2,\theta)-d(q^2,\theta)\tilde{v}_f]}{e^2Q_eQ_f},$$

$$R_{ef}(q^2,\theta)=-(q^2-M_Z^2)\frac{4\tilde{s}_e^2\tilde{c}_e^2b(q^2,\theta)d(q^2,\theta)}{e^2I_{3e}I_{3f}},$$

$$V_{ef}^{\gamma Z}(q^2,\theta)=-(q^2-M_Z^2)\frac{[a(q^2,\theta)-b(q^2,\theta)\tilde{v}_e]2\tilde{s}_e\tilde{c}_ed(q^2,\theta)}{e^2Q_eI_{3f}},$$

$$V_{ef}^{Z\gamma}(q^2,\theta)=-(q^2-M_Z^2)\frac{[c(q^2,\theta)-d(q^2,\theta)\tilde{v}_f]2\tilde{s}_e\tilde{c}_eb(q^2,\theta)}{e^2Q_fI_{3e}}. \tag{2.6}$$

In Ref. [2] and in the Appendix of Ref. [9] we gave an expression of the general polarized $e^+e^-\to\overline{ff}$ differential cross section in terms of these four functions. From this one obtains, for example, the integrated cross sections σ_f and the asymmetries $A_{FB,f}$ and $A_{LR,f}$.

To generalize our approach to the case $f=e$, Bhabha scattering, it is convenient to write the scattering amplitude at one loop as the sum of two (s-channel and t-channel) components:

$$\mathcal{A}_{ee}=\mathcal{A}_s(q^2,\theta)+\mathcal{A}_t(q^2,\theta). \tag{2.7}$$

The procedure that we have illustrated in the $e^+e^-\to\overline{ff}$ ($f\neq e$) case applies directly to the s-channel part of the Bhabha amplitude. In this case we can drop the index ef, as $e\equiv f$, and we have $V^{\gamma Z}(q^2,\theta)\equiv V^{Z\gamma}(q^2,\theta)\equiv V(q^2,\theta)$, so that we only deal with three independent functions $\tilde{\Delta}_\alpha(q^2,\theta)$, $R(q^2,\theta)$, and $V(q^2,\theta)$.

It is now straightforward to check that the same procedure can be applied step by step to the t-channel component. In full generality the latter can be written as

$$\begin{aligned}\mathcal{A}_t(q^2,\theta)=&\frac{i}{t}\overline{v}(e^+)\gamma^\mu\overline{g}_{Ve}^{(\gamma)}(q^2,\theta)v(e^+)\\&\cdot\overline{u}(e^-)\gamma_\mu\overline{g}_{Vf}^{(\gamma)}(q^2,\theta)u(e^-)+\frac{i}{t-M_Z^2}\\&\times\overline{v}(e^+)\gamma^\mu[\overline{g}_{Ve}^{(Z)}(q^2,\theta)-\overline{g}_{Ae}^{(Z)}(q^2,\theta)\gamma^5]\\&\times v(e^+)\overline{u}(e^-)\gamma_\mu[\overline{g}_{Vf}^{(Z)}(q^2,\theta)\\&-\overline{g}_{Af}^{(Z)}(q^2,\theta)\gamma^5]u(e^-),\end{aligned} \tag{2.8}$$

with the t-channel effective couplings

$$\overline{g}^{\gamma}_{Ve}(q^2,\theta)=\sqrt{4\pi\alpha(0)}Q_e\left[1+\frac{1}{2}\bar{\tilde{\Delta}}_{\alpha}(q^2,\theta)\right],$$

$$\overline{g}^{Z}_{Ve}(q^2,\theta)=\gamma_e^{1/2}I_{3e}\tilde{v}_e\left[1-\frac{1}{2}\overline{R}(q^2,\theta)-\frac{4\tilde{s}_e\tilde{c}_e}{\tilde{v}_e}|Q_f|\overline{V}(q^2,\theta)\right], \tag{2.9}$$

$$\overline{g}^{Z}_{Ae}(q^2,\theta)=\gamma_e^{1/2}I_{3e}\left[1-\frac{1}{2}\overline{R}(q^2,\theta)\right],$$

where the new functions $\bar{\tilde{\Delta}}_{\alpha}(q^2,\theta)$, $\overline{R}(q^2,\theta)$, and $\overline{V}(q^2,\theta)$ are obtained from the previous s-channel functions (without bar) by $(q^2\leftrightarrow t)$ crossing relations,

$$\bar{\tilde{\Delta}}_{\alpha}(q^2,\theta)=[\tilde{\Delta}_{\alpha}(q^2,\theta)]\left(q^2\rightarrow t=-\frac{q^2}{2}(1-\cos\theta);\right.$$

$$\left.\cos\theta\rightarrow 1+\frac{2q^2}{t}\right), \tag{2.10}$$

and analogously for $\overline{R}$ and $\overline{V}$.

The general expression of the polarized Bhabha differential cross section obtained from the sum of the s-channel [Eq. (2.1)] and t-channel [Eq. (2.8)] amplitudes is given in the Appendix, in the form

$$\frac{d\sigma}{d\cos\theta}=(1-PP')\frac{d\sigma^1}{d\cos\theta}+(1+PP')\frac{d\sigma^2}{d\cos\theta}+(P'-P)\frac{d\sigma^P}{d\cos\theta}, \tag{2.11}$$

where P and P' are the initial e^- and e^+ polarizations.

We shall write the three differential cross sections as the sum of a Born term and a one-loop contribution, $d\sigma^i=(d\sigma^i)^{Born}+(d\sigma^i)^{(1)}$.

The Born term is given by

$$\left(\frac{d\sigma^1}{d\cos\theta}\right)^{Born}=\frac{\pi\alpha^2}{q^2}\left\{\frac{t^2+u^2}{q^4}+\frac{u^2}{t^2}+\frac{2u^2}{tq^2}+2\left(\frac{3\Gamma_e}{\alpha M_Z}\right)\times\left[\frac{[u^2-t^2+\tilde{v}_e^2(u^2+t^2)](q^2-M_Z^2)}{(1+\tilde{v}_e^2)q^2[(q^2-M_Z^2)^2+M_Z^2\Gamma_Z^2]}+\frac{u^2}{q^2(t-M_Z^2)}+\frac{u^2(q^2-M_Z^2)}{t[(q^2-M_Z^2)^2+M_Z^2\Gamma_Z^2]}+\frac{u^2}{t(t-M_Z^2)}\right]+\left(\frac{3\Gamma_e}{\alpha M_Z}\right)^2\times\left[\frac{(t^2+u^2)(1+\tilde{v}_e^2)^2+4\tilde{v}_e^2(u^2-t^2)}{(1+\tilde{v}_e^2)^2[(q^2-M_Z^2)^2+M_Z^2\Gamma_Z^2]}+\frac{u^2[(1+\tilde{v}_e^2)^2+4\tilde{v}_e^2]}{(1+\tilde{v}_e^2)^2(t-M_Z^2)}\times\left(\frac{2(q^2-M_Z^2)}{[(q^2-M_Z^2)^2+M_Z^2\Gamma_Z^2]}+\frac{1}{(t-M_Z^2)}\right)\right]\right\}, \tag{2.12}$$

$$\left(\frac{d\sigma^2}{d\cos\theta}\right)^{Born}=\pi\alpha^2q^2\left\{\frac{1}{t^2}+2\left(\frac{3\Gamma_e}{\alpha M_Z}\right)\frac{(\tilde{v}_e^2-1)}{(1+\tilde{v}_e^2)t(t-M_Z^2)}+\left(\frac{3\Gamma_e}{\alpha M_Z}\right)^2\frac{(1-\tilde{v}_e^2)^2}{(1+\tilde{v}_e^2)^2(t-M_Z^2)^2}\right\}, \tag{2.13}$$

$$\left(\frac{d\sigma^P}{d\cos\theta}\right)^{Born}=\frac{4\pi\alpha^2u^2}{q^2}\left[\frac{\tilde{v}_e}{(1+\tilde{v}_e^2)}\right]\left\{\left(\frac{3\Gamma_e}{\alpha M_Z}\right)\left(\frac{1}{q^2}+\frac{1}{t}\right)\times\left[\frac{(q^2-M_Z^2)}{[(q^2-M_Z^2)^2+M_Z^2\Gamma_Z^2]}+\frac{1}{(t-M_Z^2)}\right]+\left(\frac{3\Gamma_e}{\alpha M_Z}\right)^2\left[\frac{1}{[(q^2-M_Z^2)^2+M_Z^2\Gamma_Z^2]}\times\left(1+\frac{2(q^2-M_Z^2)}{(t-M_Z^2)}\right)+\frac{1}{(t-M_Z^2)^2}\right]\right\}, \tag{2.14}$$

and the one loop contributions of the three functions can be written in a condensed way:

$$\left(\frac{d\sigma^1}{d\cos\theta}\right)^{(1)}=\frac{\pi\alpha^2}{q^2}\{(t^2+u^2)G_1(q^2,q^2)+(u^2-t^2)G_2(q^2,q^2)+u^2[G_1(t,t)+G_2(t,t)+2G_1(q^2,t)+2G_2(q^2,t)]\}, \tag{2.15}$$

$$\left(\frac{d\sigma^2}{d\cos\theta}\right)^{(1)}=\pi\alpha^2q^2[G_1(t,t)-G_2(t,t)], \tag{2.16}$$

$$\left(\frac{d\sigma^P}{d\cos\theta}\right)^{(1)}=\frac{4\pi\alpha^2u^2}{q^2}[G_3(q^2,q^2)+G_3(q^2,t)+G_3(t,q^2)+G_3(t,t)], \tag{2.17}$$

with

$$G_1(x,y)=\frac{\tilde{\Delta}_\alpha(x)+\tilde{\Delta}_\alpha(y)}{xy}+\left(\frac{3\Gamma_e}{\alpha M_Z}\right)\frac{\tilde{v}_e^2}{(1+\tilde{v}_e^2)}\left[\frac{\tilde{\Delta}_\alpha(x)-R(y)-\frac{8\tilde{s}_e\tilde{c}_e}{\tilde{v}_e}V(y)}{x(y-M_Z^2)}+\frac{\tilde{\Delta}_\alpha(y)-R(x)-\frac{8\tilde{s}_e\tilde{c}_e}{\tilde{v}_e}V(x)}{y(x-M_Z^2)}\right]-\left(\frac{3\Gamma_e}{\alpha M_Z}\right)^2$$
$$\times\left[\frac{R(x)+R(y)+\frac{8\tilde{s}_e\tilde{c}_e\tilde{v}_e}{(1+\tilde{v}_e^2)}[V(x)+V(y)]}{(x-M_Z^2)(y-M_Z^2)}\right], \tag{2.18}$$

$$G_2(x,y)=\left(\frac{3\Gamma_e}{\alpha M_Z}\right)\frac{1}{(1+\tilde{v}_e^2)}\left[\frac{\tilde{\Delta}_\alpha(x)-R(y)}{x(y-M_Z^2)}+\frac{\tilde{\Delta}_\alpha(y)-R(x)}{y(x-M_Z^2)}\right]-\left(\frac{3\Gamma_e}{\alpha M_Z}\right)^2\frac{4\tilde{v}_e^2}{(1+\tilde{v}_e^2)^2}$$
$$\times\left[\frac{R(x)+R(y)+\frac{4\tilde{s}_e\tilde{c}_e}{\tilde{v}_e}[V(x)+V(y)]}{(x-M_Z^2)(y-M_Z^2)}\right], \tag{2.19}$$

$$G_3(x,y)=\frac{\tilde{v}_e}{(1+\tilde{v}_e^2)}\left\{\left(\frac{3\Gamma_e}{\alpha M_Z}\right)\frac{\tilde{\Delta}_\alpha(x)-R(y)-\frac{4\tilde{s}_e\tilde{c}_e}{\tilde{v}_e}V(y)}{x(y-M_Z^2)}-\left(\frac{3\Gamma_e}{\alpha M_Z}\right)^2\left[\frac{R(x)+R(y)+\frac{4\tilde{s}_e\tilde{c}_e}{\tilde{v}_e}V(x)+\frac{8\tilde{s}_e\tilde{c}_e\tilde{v}_e}{(1+\tilde{v}_e^2)}V(y)}{(x-M_Z^2)(y-M_Z^2)}\right]\right\}, \tag{2.20}$$

where we use a condensed notation (for x and y corresponding to q^2 or t) $\tilde{\Delta}_\alpha(q^2)$, meaning $\tilde{\Delta}_\alpha(q^2,\theta)$, and $\tilde{\Delta}_\alpha(t)$, meaning $\tilde{\Delta}_\alpha(q^2,\theta)$; we use a similar notation for R and V.

From the three previous quantities $d\sigma^{1,2,P}$, we can compute, for instance, the unpolarized angular distribution

$$\frac{d\sigma}{d\cos\theta}\equiv\frac{d\sigma^1}{d\cos\theta}+\frac{d\sigma^2}{d\cos\theta}, \tag{2.21}$$

the left-right polarization asymmetry

$$A_{LR}(q^2,\theta)=\left[\frac{d\sigma^P}{d\cos\theta}\right]\Big/\left[\frac{d\sigma}{d\cos\theta}\right], \tag{2.22}$$

and the new $(LL+RR)/(LR+RL+LL+RR)$ polarization asymmetry which arises from the typical t-channel scattering amplitude:

$$A_{||}(q^2,\theta)=\left[\frac{d\sigma^2}{d\cos\theta}\right]\Big/\left[\frac{d\sigma}{d\cos\theta}\right]. \tag{2.23}$$

III. APPLICATIONS TO SEVERAL NP MODELS

A. Universal NP with a high scale

The previous representation [Eqs. (2.15)–(2.20)] continues to be valid in the presence of (NP) that does not add extra Lorentz structures to those of the SM. In this case, one simply decomposes the three general one-loop functions as

$$\tilde{\Delta}_\alpha,R,V=(\tilde{\Delta}_\alpha,R,V)^{SM}+(\tilde{\Delta}_\alpha,R,V)^{NP}, \tag{3.1}$$

and computes the (NP) effects on the various observables, once their contribution to $(\tilde{\Delta}_\alpha,R,V)$ is specified.

For a model of new physics that does not satisfy special simplicity requests, the calculation of virtual effects in the Bhabha scattering is affected by a proliferation of terms with respect to the annihilation process $e^+e^-\to f\bar{f}$, $(f\neq e)$, as one sees immediately from inspection of Eqs. (2.15)–(2.20). In fact, after θ integration, one will find in general a set of different functions of q^2 that correspond to each power of θ in the integrand. Each set arises from the *six* original functions $\tilde{\Delta}_\alpha$, $\bar{\tilde{\Delta}}_\alpha$, R, $\bar{R}$, V, and $\bar{V}$, which means to double the corresponding number of the case $f\neq e$. Although this can be a purely computational problem, it obviously complicates the practical treatment for this process.

The situation shows a drastic change for those models of new physics that satisfy the requests of being, at the same time, universal, independent of the s and t channels scattering angle (e.g., only contributing self-energies and/or vertices), and endowed with an intrinsic scale Λ ''sufficiently'' larger than $\sqrt{q^2}$. In fact, in the Z-peak subtracted approach, one has, by construction,

$$\tilde{\Delta}_\alpha(0,\theta)=\bar{\tilde{\Delta}}_\alpha(0,\theta)=R(M_Z^2,\theta)=\bar{R}(M_Z^2,\theta)=V(M_Z^2,\theta)$$
$$=\bar{V}(M_Z^2,\theta)=0. \tag{3.2}$$

For universal new physics (UNP) effects of the previously considered type, one can then write the parametrization

$$R^{UNP}(z)=\frac{(z-M_Z^2)}{M_Z^2}[\delta_Z], \tag{3.3}$$

$$V^{UNP}(z)=\frac{(z-M_Z^2)}{M_Z^2}[\delta_s], \tag{3.4}$$

$$\tilde{\Delta}_\alpha^{UNP}(z)=\frac{z}{M_Z^2}[\delta_\gamma], \tag{3.5}$$

where $z=q^2,t$.

The quantities $\delta_{Z,s,\gamma}$ will be in general unknown functions of z. For $\Lambda^2 \gg z$ we can reasonably assume that the three functions are smooth. This means that they could be well approximated by the coefficient of the *lowest* power in a q^2 expansion that is $\delta_i(0)$ whenever $\delta_i(0)\neq 0$ (this will be the case in the two considered examples). In this case, the *same* three parameters will describe the NP effects both on the *s*- and *t*-channel observables. These parameters are also the same that appear, for the chosen models, in all the remaining proccesses $e^+e^-\to f\bar{f}$ $(f\neq e)$. This fact allows one to combine the theoretical analysis of the two types of processes *without an increase of parameters*, thus improving the accuracy of the conclusions that are reached.

The NP expression of the functions $G_i(x,y)$ in this case acquires the simple form

$$\begin{aligned}G_1^{UNP}(x,y)=\frac{1}{M_Z^2}\Bigg\{&\delta_\gamma\left[\frac{1}{x}+\frac{1}{y}\right]+\left(\frac{3\Gamma_e}{\alpha M_Z}\right)\left(\frac{\tilde{v}_e^2}{1+\tilde{v}_e^2}\right)\\&\times\Bigg[\delta_\gamma\left(\frac{1}{x-M_Z^2}+\frac{1}{y-M_Z^2}\right)-\left(\delta_Z+\frac{8\tilde{s}_e\tilde{c}_e}{\tilde{v}_e}\delta_s\right)\\&\times\left(\frac{1}{x}+\frac{1}{y}\right)\Bigg]-\left(\frac{3\Gamma_e}{\alpha M_Z}\right)^2\Bigg[\delta_Z+\left(\frac{8\tilde{s}_e\tilde{c}_e\tilde{v}_e}{1+\tilde{v}_e^2}\right)\delta_s\Bigg]\\&\times\left[\frac{1}{x-M_Z^2}+\frac{1}{y-M_Z^2}\right]\Bigg\},\end{aligned} \tag{3.6}$$

$$\begin{aligned}G_2^{UNP}(x,y)=\frac{1}{M_Z^2}\Bigg\{&\left(\frac{3\Gamma_e}{\alpha M_Z}\right)\left(\frac{1}{1+\tilde{v}_e^2}\right)\Bigg[\delta_\gamma\left(\frac{1}{x-M_Z^2}+\frac{1}{y-M_Z^2}\right)\\&-\delta_Z\left(\frac{1}{x}+\frac{1}{y}\right)\Bigg]-\left(\frac{3\Gamma_e}{\alpha M_Z}\right)^2\frac{4\tilde{v}_e^2}{(1+\tilde{v}_e^2)^2}\\&\times\left(\delta_Z+\frac{4\tilde{s}_e\tilde{c}_e}{\tilde{v}_e}\delta_s\right)\left(\frac{1}{x-M_Z^2}+\frac{1}{y-M_Z^2}\right)\Bigg\},\end{aligned} \tag{3.7}$$

$$\begin{aligned}G_3^{UNP}(x,y)=\frac{1}{M_Z^2}\frac{\tilde{v}_e}{1+\tilde{v}_e^2}\Bigg\{&\left(\frac{3\Gamma_e}{\alpha M_Z}\right)\Bigg[\frac{\delta_\gamma}{y-M_Z^2}\\&-\frac{\delta_Z+\frac{4\tilde{s}_e\tilde{c}_e}{\tilde{v}_e}\delta_s}{x}\Bigg]-\left(\frac{3\Gamma_e}{\alpha M_Z}\right)^2\\&\times\Bigg[\frac{\delta_Z+\frac{4\tilde{s}_e\tilde{c}_e}{\tilde{v}_e}\delta_s}{y-M_Z^2}+\frac{\delta_Z+\frac{8\tilde{s}_e\tilde{c}_e\tilde{v}_e}{(1+\tilde{v}_e^2)}\delta_s}{x-M_Z^2}\Bigg]\Bigg\},\end{aligned} \tag{3.8}$$

The three constants δ_Z, δ_s, and δ_γ depend on the chosen model, and can be easily determined in each separate case. To show how this procedure works in practice, we shall provide the expressions of the δ_i in a couple of specific cases that meet our simplicity requests. With this aim, we have considered the following models.

(1) *Anomalous gauge couplings (AGC's).* We used the framework of Ref. [10], in which the effective Lagrangian is constructed with dimension six operators respecting $SU(2)\times U(1)$ and *CP* invariance. As shown in Ref. [4], only two parameters (f_{DW} and f_{DB}) survive in the *Z*-peak subtracted approach. The explicit expressions of the UNP contribution to δ_Z, δ_s, and δ_γ are

$$\begin{aligned}\delta_Z&=8\pi\alpha\left(\frac{M_Z^2}{\Lambda^2}\right)\left(\frac{\tilde{c}_e^2}{\tilde{s}_e^2}f_{DW}+\frac{\tilde{s}_e^2}{\tilde{c}_e^2}f_{DB}\right),\\\delta_s&=8\pi\alpha\left(\frac{M_Z^2}{\Lambda^2}\right)\left(\frac{\tilde{c}_e}{\tilde{s}_e}f_{DW}-\frac{\tilde{s}_e}{\tilde{c}_e}f_{DB}\right),\\\delta_\gamma&=-8\pi\alpha\left(\frac{M_Z^2}{\Lambda^2}\right)(f_{DW}+f_{DB}).\end{aligned} \tag{3.9}$$

They satisfy the linear constraint

$$\delta_Z-\frac{1-2\tilde{s}_e^2}{\tilde{s}_e\tilde{c}_e}\delta_s+\delta_\gamma=0. \tag{3.10}$$

(2) *Technicolor* (TC). The second considered model was one of technicolor type, with two families of strongly coupled resonances (V and A) [5]. The typical UNP parameters are the two ratios F_A/M_A and F_V/M_V, where $F_{A,V}$ and $M_{A,V}$ are the couplings and the masses (that in this case play the role of the new physics scale $\Lambda^{TC}\gg q^2$) of the *lightest* axial and vector resonances. The contributions to δ_Z, δ_s, and δ_γ are

$$\delta_Z=\frac{\pi\alpha}{\tilde{s}_e^2\tilde{c}_e^2}\left[(1-2\tilde{s}_e^2)^2\frac{M_Z^2}{M_V^4}F_V^2+\frac{M_Z^2}{M_A^4}F_A^2\right],$$

$$\delta_s=\frac{2\pi\alpha}{\tilde{s}_e\tilde{c}_e}(1-2\tilde{s}_e^2)\frac{M_Z^2}{M_V^4}F_V^2,$$

$$\delta_\gamma=-4\pi\alpha\left(\frac{M_Z^2}{M_V^4}\right)F_V^2. \tag{3.11}$$

Again, we have a linear constraint in the $(\delta_Z,\delta_s,\delta_\gamma)$ space,

$$\delta_s=-\left(\frac{1-2\tilde{s}_e^2}{2\tilde{s}_e\tilde{c}_e}\right)\delta_\gamma, \tag{3.12}$$

and the conditions

$$\delta_{Z,s}>0, \quad \delta_\gamma<0 \tag{3.13}$$

B. Nonuniversal examples

Strictly speaking, our procedure has been motivated by the possibility of investigating models of a special universal type, for which the number of parameters to be determined can be suitably reduced. But there exist interesting models of NP that, although not of universal type, can be nevertheless described by a very restricted number of parameters. In these special simple cases our Z-peak subtracted procedure can be applied, without invoking any smoothness assumption, using the more general expressions of Eqs. (2.15)–(2.20). In what follows, we have considered two cases that seem to us particularly relevant. These are:

(3) *Contact terms.* With the idea of compositeness (but it applies to any virtual NP effect with a high intrinsic scale, for example higher vector boson exchanges, satisfying chirality conservation), the interaction

$$\mathcal{L}=k_{if}\frac{4\pi}{\Lambda^2}\{\eta_{LL}(\bar{\Psi}_L^i\gamma^\mu\Psi_L^i)(\bar{\Psi}_L^f\gamma_\mu\Psi_L^f)+\eta_{RR}(\bar{\Psi}_R^i\gamma^\mu\Psi_R^i)\times(\bar{\Psi}_R^f\gamma_\mu\Psi_R^f)+\eta_{RL}(\bar{\Psi}_R^i\gamma^\mu\Psi_R^i)(\bar{\Psi}_L^f\gamma_\mu\Psi_L^f)+\eta_{LR}(\bar{\Psi}_L^i\gamma^\mu\Psi_L^i)(\bar{\Psi}_R^f\gamma_\mu\Psi_R^f)\} \tag{3.14}$$

was first introduced in Ref. [11] for any four-fermion interaction ($i\bar{i}\to f\bar{f}$); $k_{if}=\frac{1}{2}$ for $i\equiv f$, $k_{if}=1$ otherwise, $\Psi_L=(1-\gamma^5)/2\Psi$, $\Psi_R=(1+\gamma^5)/2\Psi$, and η_{ab} are phase factors defining the chirality structure of the interaction. Various applications have been made for pure chiral cases $(ij)=LL$ or RR or LR or RL (keeping only one $\eta_{ij}=\pm1$), as well as for mixed cases like VV ($\eta_{LL}=\eta_{RR}=\eta_{RL}=\eta_{LR}=\pm1$), AA ($\eta_{LL}=\eta_{RR}=-\eta_{RL}=-\eta_{LR}=\pm1$), VA ($\eta_{LL}=-\eta_{RR}=\eta_{RL}=-\eta_{LR}=\pm1$), and AV ($\eta_{LL}=-\eta_{RR}=-\eta_{RL}=\eta_{LR}=\pm1$); see Ref. [12] for a general discussion.

In the Z-peak subtracted representation, the effect of this interaction on the $e^+e^-\to f\bar{f}$ $(f\neq e)$ observables is obtained through the following expressions:

$$\tilde{\Delta}_{\alpha,ef}(q^2,\theta)=\left(\frac{\pi q^2}{e^2Q_eQ_f\Lambda^2}\right)[\eta_{LL}(1-v_e)(1-v_f)+\eta_{RR}(1+v_e)(1+v_f)+\eta_{RL}(1+v_e)(1-v_f)+\eta_{LR}(1-v_e)(1+v_f)],$$

$$R_{ef}(q^2,\theta)=-\left(\frac{4\tilde{s}_e^2\tilde{c}_e^2\pi(q^2-M_Z^2)}{e^2I_{3e}I_{3f}\Lambda^2}\right)\times[\eta_{LL}+\eta_{RR}-\eta_{RL}-\eta_{LR}],$$

$$V_{ef}^{\gamma Z}(q^2,\theta)=-\left(\frac{2\tilde{s}_e\tilde{c}_e\pi(q^2-M_Z^2)}{e^2Q_eI_{3f}\Lambda^2}\right)[\eta_{LL}(1-v_e)-\eta_{RR}(1+v_e)+\eta_{RL}(1+v_e)-\eta_{LR}(1-v_e)],$$

$$V_{ef}^{Z\gamma}(q^2,\theta)=-\left(\frac{2\tilde{s}_e\tilde{c}_e\pi(q^2-M_Z^2)}{e^2Q_fI_{3e}\Lambda^2}\right)[\eta_{LL}(1-v_f)-\eta_{RR}(1+v_f)-\eta_{RL}(1-v_f)+\eta_{LR}(1+v_f)]. \tag{3.15}$$

For each choice of chirality structure, like LL, RR, LR, RL, VV, AA, VA, and AV, the effects on the differential cross section for two fermion production can be described by a single parameter Λ.

In the case of Bhabha scattering, the constraint $\eta_{RL}=\eta_{LR}$ applies, so that the above expression can be put in the forms of Eqs. (3.3)–(3.5), with

$$\delta_Z=-\left(\frac{16\tilde{s}_e^2\tilde{c}_e^2\pi M_Z^2}{e^2\Lambda^2}\right)[\eta_{LL}+\eta_{RR}-2\eta_{LR}]$$

$$\delta_s=-\left(\frac{4\tilde{s}_e\tilde{c}_e\pi M_Z^2}{e^2\Lambda^2}\right)[\eta_{LL}(1-v_e)-\eta_{RR}(1+v_e)+2v_e\eta_{LR}], \tag{3.16}$$

$$\delta_\gamma=\left(\frac{\pi M_Z^2}{e^2\Lambda^2}\right)[\eta_{LL}(1-v_e)^2+\eta_{RR}(1+v_e)^2+2\eta_{LR}(1-v_e^2)].$$

(4) *Extra dimensions.* Recently, intense activity has developed concerning the possible low-energy effects of graviton exchange. The following matrix element for the four-fermion process $e^+e^-\to\bar{f}f$ [13] is predicted:

$$\frac{\lambda}{\Lambda^4}[\bar{e}\gamma^\mu e\bar{f}\gamma_\mu f(p_2-p_1)\cdot(p_4-p_3)-\bar{e}\gamma^\mu e\bar{f}\gamma^\nu f(p_2-p_1)_\nu(p_4-p_3)_\mu] \tag{3.17}$$

For this model, in the case of Bhabha scattering, one finds the following contributions to $\delta_{\gamma,Z,s}$ that, as one sees, are now genuine q^2,θ functions:

TABLE I. LEP2. 95% C.L. bounds on $\delta_{s,Z,\gamma}$, resulting from a global fit of combined LEP2 data. In the first column, the observables included in the fit are $\sigma_{\mu,\tau}$, $A_{FB,\mu,\tau}$, σ_5 and measured at 183 and 189 GeV. In the second column, we add the Bhabha unpolarized differential cross section (in nine intervals of the cosine of the scattering angle) at 189 GeV. The last two columns show the improvement of the bounds when only the forward (backward) Bhabha scattering measurements are included.

	Without Bhabha	With all Bhabha	Forward	Backward
δ_Z	-0.001 ± 0.031	0.0064 ± 0.028	0.006 ± 0.03	0.0011 ± 0.029
δ_s	-0.004 ± 0.032	-0.0087 ± 0.031	-0.0084 ± 0.032	-0.0057 ± 0.031
δ_γ	-0.0022 ± 0.0083	0.00019 ± 0.0074	0.00014 ± 0.0075	-0.0019 ± 0.0081

$$\delta_\gamma=\left(\frac{\lambda q^2 M_Z^2}{\Lambda^4}\right)\frac{(\tilde{v}_e^2-2\cos\theta)}{e^2},$$

$$\delta_Z=-\left(\frac{\lambda q^2 M_Z^2}{\Lambda^4}\right)\left(\frac{16\tilde{s}_e^2\tilde{c}_e^2}{e^2}\right), \tag{3.18}$$

$$\delta_s=\left(\frac{\lambda q^2 M_Z^2}{\Lambda^4}\right)\left(\frac{4\tilde{s}_e\tilde{c}_e\tilde{v}_e}{e^2}\right).$$

Illustrations will be given in Sec. IV with the normalization $\lambda=\pm1$. Note that the q^2 factor is purely kinematical, and a consequence of the higher dimension of the interaction Lagrangian. Note also the presence of a term proportional to $q^2\cos\theta$ in the s-channel photon coefficient δ_γ, which gives a contribution proportional to $t+2q^2$ in the t channel, according to Eq. (2.10). This contribution will turn out to have the largest effect through the interference with the standard photon exchange amplitude.

Our theoretical description of new physics effects is at this point concluded. Section IV will be devoted to a detailed numerical analysis of the information that can be derived on the involved parameters by the present (LEP2) and future, using both Bhabha scattering and all the remaining $e^+e^-\to\bar{f}f$ processes.

IV. NUMERICAL RESULTS

A. LEP2 (present and future)

As a first application of our approach, we have used some of the LEP2 results on fermion pair production in order to constrain the set of constants $\delta_{Z,s,\gamma}$ which fully describes the effects of general universal new physics. In particular, in the same spirit of a previous study [6], we have considered the following ''non-Bhabha'' observables: $\sigma_{\mu,\tau}$ (the cross section for μ and τ pair production), $A_{FB,\mu,\tau}$ (the related forward-backward asymmetries), and σ_5 (the cross section for production of quark pairs, for the five light flavors accessible at LEP energies). In addition to these observables we have included the unpolarized differential Bhabha cross section, measured in intervals of the cosine of the polar angle of the scattered electron. For the muon and tau cross sections and asymmetries and for the hadronic cross section, combinations of preliminary results of the four LEP experiments with the data collected at center of mass energies of 183 and 189 GeV have been used [14]. Although based on preliminary results, the combined measurements allow one to take advantage of the whole data sample produced at LEP2, and therefore to benefit from the reduced statistical error and from the proper treatment of the various sources of experimental systematic uncertainty. A measurement of the differential cross section for Bhabha scattering with a collinearity smaller that 10° has been recently performed with a data sample of approximately 180 pb^{-1} at a center-of-mass energy of 189 GeV [15]. The differential cross section is measured in nine uniform intervals of the polar angle of the scattered electron, $\cos\theta_{e^-}$, in the range $(-0.9, 0.9)$. The precision of the measurement, which is limited primarily by the statistical uncertainty, reaches the level of 1% in the interval of most forward scattering angles.

This measurement, together with the combined results on muon, tau, and hadronic observables, has been compared to the standard model prediction corresponding to the experimental signal definition. The deviations of the measurement with respect to the standard model expectations have then been used to measure and constrain the parameters δ_Z, δ_s, and δ_γ, with a χ^2 fit. In the fit procedure the uncertainty on the reference standard model prediction itself must be taken into account. The theoretical uncertainties on the standard model predictions for fermion pair production at LEP2 energies are mainly related to the estimate of the large QED corrections. In the case of $\mu^+\mu^-$, $\tau^+\tau^-$, and $q\bar{q}$ production, the differences between predictions of several semianalytic or Monte Carlo calculations [16–18] for cross sections and asymmetries are smaller than 1% and, therefore, they are negligible with respect to the experimental error. In the Bhabha scattering process the different programs [17,19,20] providing the standard model predictions compare with each other at the level of 2% in the experimental acceptance. Therefore, in our study, we have assigned a 2% uncertainty to the reference standard model prediction for the Bhabha differential cross section. This uncertainty reflects an error larger than the experimental one in the region of forward scattering, which, as will be discussed in the following, is the most sensitive to new physics effects in δ_γ.

The results of the analysis are shown in Table I. As one sees, the addition of Bhabha scattering improves, although not spectacularly, the bound on δ_γ which is constrained by

TABLE II. LEP2. 95% C.L. bounds on $\delta_{s,Z,\gamma}$, resulting from a global fit of the simulated forthcoming combined LEP2 data. The observables included in the fit are $\sigma_{\mu,\tau}$, $A_{FB,\mu,\tau}$, and σ_5 at 183, 189, and 200 GeV, and, in the second column, the nine angular measurements of the Bhabha unpolarized cross section at 189 and 200 GeV. For all the observables we assume that the measurements are coincident with the standard model predictions. The errors are the experimental ones at 183 and 189 GeV. At 200 GeV, the errors are the statistical ones associated with a 400-pb^{-1} integrated luminosity per experiment with or without (second and third columns) a 2% theoretical error on Bhabha scattering.

	Without Bhabha	With all Bhabha and 2% th. err	With all Bhabha
δ_Z	0.014	0.012	0.012
δ_s	0.015	0.013	0.013
δ_γ	0.0038	0.0034	0.0028

the data in the forward-scattering angle region, where the Bhabha cross section is dominated by the *t*-channel photon exchange contribution. It is interesting to take in mind that, at present, the sensitivity to NP effects in the forward Bhabha cross section is spoiled by the theoretical uncertainty on the standard model theoretical prediction, which dominates over the experimental error. Should this error be reduced, the role of this measurement would certainly be more relevant.

To give a more quantitative meaning to the latter claim, we have simulated a forthcoming measurement at 200 GeV with an overall 400-pb^{-1} luminosity for each experiment, and repeated the previous analysis adding these future data to those available at 183 and 189 GeV. For consistency, we have assumed in all three sets of data a central value coincident with the SM prediction. The errors are those available at 183 and 189 GeV. At 200 GeV we considered two scenarios, one with purely statistical errors and one with their combination with a 2% theoretical error on Bhabha scattering. The difference between the two cases mainly affects the forward-scattering cone and therefore δ_γ. The results of this second analysis are shown in Table II. As one sees, in agreement with the qualitative expectations, the role of Bhabha scattering is now definitely more relevant in the determination of the bound for the photonic parameter δ_γ.

TABLE III. LEP2. Bounds on a nonuniversal new physics scale at 95% C.L. resulting from a global fit of the present combined LEP2 data. We consider the models of contact interactions (in the eight cases *LL*, *RR*, *LR*, *RL*, *VV*, *AA*, *AV*, and *VA*) and extra dimensions discussed in the paper. The data sets used for the fit are the same as in Table I. Since the central value for $1/\Lambda$ is not zero, we show the two different bounds for $|\Lambda|$ that are obtained in the two cases $\Lambda<0$ and $\Lambda>0$, respectively.

	Without Bhabha	With all Bhabha	Forward	Backward
Λ_{LL}	10–9.9	11–9.2	11–9.2	10–9.8
Λ_{RR}	7.7–12	8.7–10	8.7–10	7.8–12
Λ_{LR}	6.5–9.2	16–7.8	14–7.3	8.2–9.2
Λ_{RL}	7.2–15	12–9.7	11–9.5	8.3–13
Λ_{VV}	13–20	17–16	16–16	13–20
Λ_{AA}	16–13	14–14	14–14	15–13
Λ_{AV}	17–8.7	17–8.7	17–8.7	17–8.7
Λ_{VA}	4–3.3	4.2–3.2	4.2–3.2	4–3.3
Λ_{ED}	0.69–0.75	0.82–2.2	0.8–1.9	0.77–0.9

The same two analyses have been performed for the two models involving contact terms and extra dimensions. The results are presented in Tables III and IV. For what concerns the contact terms, one should first note that the values of the bounds obtained from $e^+e^-\to\mu^+\mu^-,q\bar{q}$ (without Bhabha scattering) depend strongly on the chirality structure. This comes from the interference of the contact amplitude with the standard γ and Z exchange amplitudes, which is larger when the chirality structures of both amplitudes are close to each other. In particular the *VA* bound is found very low, because the standard *VA* amplitude is depressed by the small Ze^+e^- vector coupling. One then sees that the effect of the Bhabha process on these bounds is generally modest. An opposite situation appears for the case of extra dimensions, where the bulk of the effect is provided by the ''forward'' data. As already mentioned in Sec. III B [see (4)], the largest effect on the differential cross section comes from the interference of the standard photon exchange with the extra dimension terms both in the *t* channel, followed by a term in mixed *s* and *t* channels; the term in two *s* channels is much smaller. Once again, this is more clearly visible in the analysis that uses the future data at 200 GeV; in this case one assumes no theoretical error in the Bhabha component.

All the numerical results exhibited in Tables I and II can be represented graphically. In Figs. 1 and 2 we show the planar ellipses that are obtained by projecting onto the three planes (δ_s,δ_γ), (δ_Z,δ_γ), and (δ_Z,δ_s) the 95% C.L. allowed three-dimensional region resulting from a global fit of all data in terms of the three parameters $\delta_{Z,s,\gamma}$. For completeness, we also show the results for the two representative AGC and TC models. As a very preliminary comment concerning the latter cases, we can note that, although at a rather qualitative level, LEP2 data apparently do not particularly support the considered TC theoretical proposal that would require $\delta_s>0$.

B. LC analyses

This analysis has been performed in a spirit that is very similar to that used for the future 200-GeV LEP2 analyses.

TABLE IV. LEP2. Bounds on a nonuniversal new physics scale at 95% C.L. resulting from a global fit of the simulated forthcoming combined final LEP2 data. Data sets are chosen as in Table II.

	Without Bhabha	With all Bhabha and 2% th. err	With all Bhabha
Λ_{LL}	15	15	16
Λ_{RR}	13	14	15
Λ_{LR}	11	16	18
Λ_{RL}	13	17	18
Λ_{VV}	22	24	27
Λ_{AA}	21	21	22
Λ_{AV}	16	16	16
Λ_{VA}	5.2	5.2	5.3
Λ_{ED}	0.89	1.2	1.4

In other words, we have assumed a set of measurements at $\sqrt{q^2}=500$ GeV whose central values agree with the SM predictions, and postulated a purely statistical error corresponding to a high luminosity of 500 fb^{-1}. We have added to the previous LEP2 ''non-Bhabha'' observables the longitudinal polarization asymmetry A_{LR} for lepton production. A discussion of the important role of this observable can be found in Ref. [21]. Of course, in principle other measurements, e.g., for final b or t quarks could be used. We have also assumed nine angular Bhabha measurements for all the three different observables (σ, σ^1, and σ^P) defined in Sec. II. More precisely, in each bin $[\theta_{min},\theta_{max}]$, we have considered

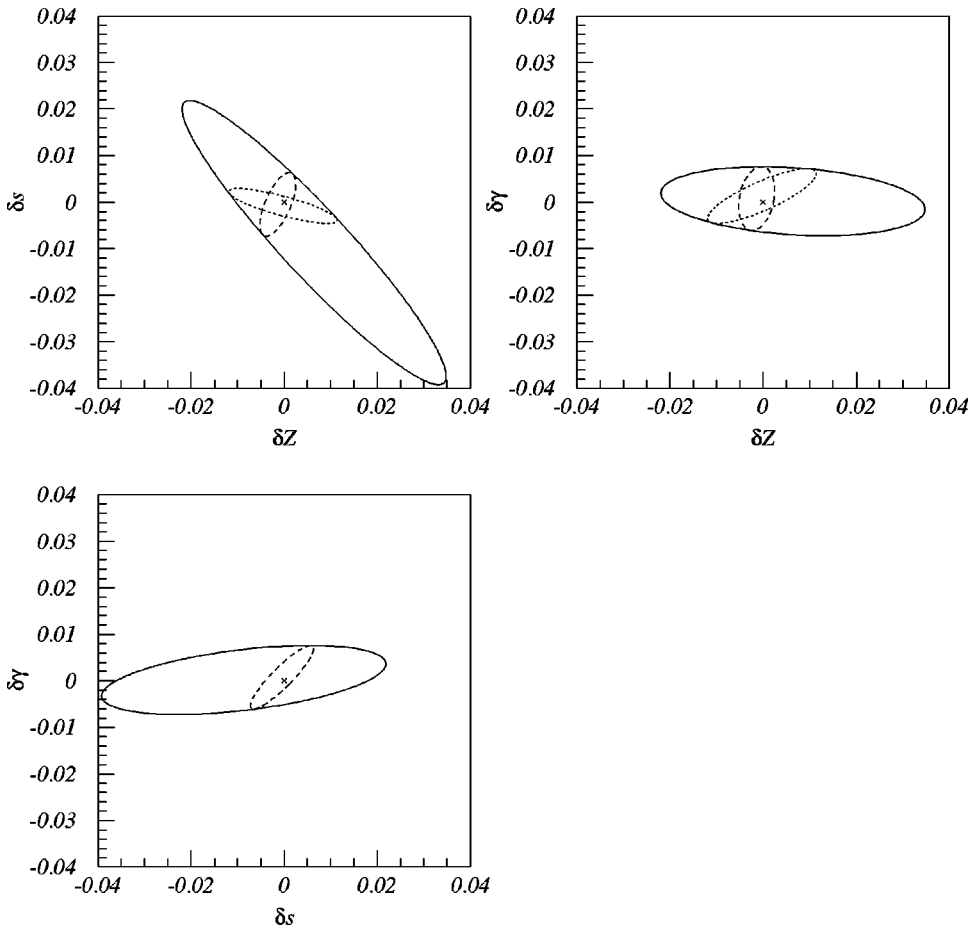

FIG. 1. Two-dimensional projections of the 95% C.L. allowed region in the $\delta_{s,Z,\gamma}$ space from a global fit of LEP2 results on two fermion production. The observables included in the fit are $\sigma_{\mu,\tau}$, $A_{FB,\mu,\tau}$, and σ_5 measured at 183 and 189 GeV, and the Bhabha unpolarized differential cross section (in nine intervals of the cosine of the scattering angle) at 189 GeV. The inner ellipses are the projection of the intersection of the three-dimensional ellipse and the AGC (dashed line) or TC (dotted line) constraints. The small cross marks the axes origin, corresponding to the standard model case.

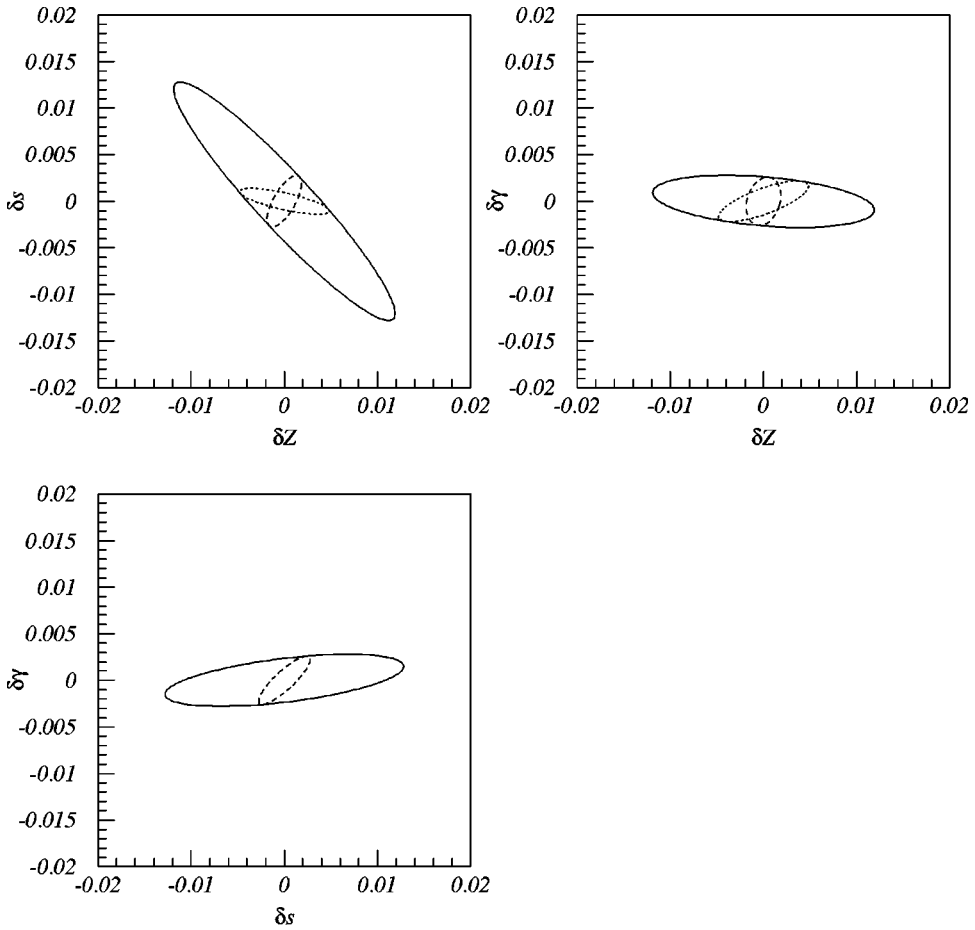

FIG. 2. Two-dimensional projections of the 95% C.L. allowed region in the $\delta_{s,Z,\gamma}$ space from a global fit of LEP2 results on two fermion production. The observables included in the fit are $\sigma_{\mu,\tau}$, $A_{FB,\mu,\tau}$, and σ_5 measured at 183, 189, and 200 GeV, and the nine angular measurements of the Bhabha unpolarized cross section at 189 and 200 GeV. We always assumed the experimental measurements to be coincident with the standard model predictions. About the errors, we took the available actual experimental errors for measurements at 183 and 189 GeV (as in Fig. 1) and a purely statistical error at 200 GeV under the assumption of an integrated luminosity of 400 pb^{-1} for each of the four LEP2 experiments. The inner ellipses are the projection of the intersection of the three dimensional ellipse and the AGC (dashed line) or TC (dotted line) constraints.

$$\sigma_{[\theta_{min},\theta_{max}]}=\int_{\cos\theta_{max}}^{\cos\theta_{min}}\frac{d\sigma}{d\cos\theta}d\cos\theta, \tag{4.1}$$

$$A_{LR,[\theta_{min},\theta_{max}]}=\frac{1}{\sigma_{[\theta_{min},\theta_{max}]}}\int_{\cos\theta_{max}}^{\cos\theta_{min}}\frac{d\sigma^P}{d\cos\theta}d\cos\theta, \tag{4.2}$$

$$A_{||,[\theta_{min},\theta_{max}]}=\frac{1}{\sigma_{[\theta_{min},\theta_{max}]}}\int_{\cos\theta_{max}}^{\cos\theta_{min}}\frac{d\sigma^2}{d\cos\theta}d\cos\theta, \tag{4.3}$$

Tables V and VI contain numerical results for universal and nonuniversal models. As a general feature, one notices that in the universal case the limits on *all* three parameters $\delta_{Z,s,\gamma}$ are substantially (a factor of 2) improved by the use of Bhabha observables. The interesting feature is that, in each case, different Bhabha observables play the crucial role. In fact, δ_Z is mostly affected by $A_{||}$ (in both angular directions), δ_s (as one expects) is most affected by A_{LR} (in the forward cone), and δ_γ is most affected by the unpolarized σ (again, for very small angles). In the considered nonuniversal cases, the effect is, again, not spectacular (although not negligible) for the contact terms. Quite the contrary, there would be a large (a factor 2) effect in the case of extra dimensions, mostly due to the unpolarized cross section at small angles. For this specific model of new physics, Bhabha scattering therefore seems to represent a fundamental experimental measurement. This statement is well in agreement with the results of a recent numerical analysis of LEP2 data [22].

V. CONCLUSION

In conclusion, we have shown that, for a class of theoretical models of new physics that is certainly not empty, the generalization of the *Z*-peak subtracted approach to the case of Bhabha scattering can be simply performed, leading in general to improvements of the information that might be obtained. As a general statement, Bhabha scattering always appears to be relevant; for models of universal type, polarized and unpolarized observables play a crucial role in the determination of the bounds for the different parameters; in other nonuniversal interesting cases, such as, in particular, that of extra dimensions, unpolarized Bhabha observables appear to play a fundamental role.

APPENDIX: GENERAL FORM OF THE POLARIZED BHABHA SCATTERING CROSS SECTION

$$\frac{d\sigma}{d\cos\theta}=(1-PP')\frac{d\sigma^1}{d\cos\theta}+(1+PP')\frac{d\sigma^2}{d\cos\theta}+(P'-P)\frac{d\sigma^P}{d\cos\theta}, \tag{A1}$$

with

TABLE V. Linear collider. 95% C.L. bounds on $\delta_{s,Z,\gamma}$ resulting from a global fit of LC data assuming that data are taken at 500 GeV with an integrated high luminosity 500 fb^{-1}. The ''non-Bhabha'' observables included in the fit are σ_l, $A_{FB,l}$, $A_{LR,l}$, and σ_5, where l stands for a lepton. The ''Bhabha'' observables are the unpolarized angular distribution and the two asymmetries A_{LR} and $A_{||}$ defined in the paper. Each of these three observables is assumed to be measured in the same nine bins as in the LEP2 analysis. The central values are assumed to coincide with the standard model predictions, and the errors are purely statistical. The first column is obtained without including the Bhabha observables in the fit. The second column is with all the Bhabha observables. The next three columns are obtained including in the fit only one of the three σ, A_{LR}, and $A_{||}$. Finally, the last two columns are obtained by using the three observables, but only in the forward (backward) cone.

	Without Bhabha	With all Bhabha	σ	A_{LR}	$A_{\|\|}$	forw.	back.
10^4 δ_Z	2.4	1.3	1.9	2.1	1.7	1.6	1.7
10^4 δ_s	1.4	0.8	1.3	0.85	1.3	0.82	1.3
10^4 δ_γ	1.1	0.56	0.62	1.1	0.9	0.65	0.82

$$\frac{d\sigma^{N1}}{d\cos\theta}=\frac{1}{16\pi q^2}\left\{\frac{t^2+u^2}{q^4}(g_{Ve}^{(\gamma)})^4+\frac{2(q^2-M_Z^2)}{q^2[(q^2-M_Z^2)^2+M_Z^2\Gamma_Z^2]}[(t^2+u^2)(g_{Ve}^{(\gamma)}g_{Ve}^{(Z)})^2+(u^2-t^2)(g_{Ve}^{(\gamma)}g_{Ae}^{(Z)})^2]\right.$$
$$+\frac{1}{[(q^2-M_Z^2)^2+M_Z^2\Gamma_Z^2]}[(t^2+u^2)[(g_{Ve}^{(Z)})^2+(g_{Ae}^{(Z)})^2]+4(u^2-t^2)(g_{Ve}^{(Z)}g_{Ae}^{(Z)})^2]+\frac{2u^2}{q^2t}(g_{Ve}^{(\gamma)}\overline{g}_{Ve}^{(\gamma)})^2$$
$$+\frac{2u^2}{q^2(t-M_Z^2)}(g_{Ve}^{(\gamma)})^2[(\overline{g}_{Ve}^{(Z)})^2+(\overline{g}_{Ae}^{(Z)})^2]+\frac{2u^2(q^2-M_Z^2)}{t[(q^2-M_Z^2)^2+M_Z^2\Gamma_Z^2]}(\overline{g}_{Ve}^{(\gamma)})^2[(g_{Ve}^{(Z)})^2+(g_{Ae}^{(Z)})^2]$$
$$+\frac{2u^2(q^2-M_Z^2)}{(t-M_Z^2)[(q^2-M_Z^2)^2+M_Z^2\Gamma_Z^2]}([(g_{Ve}^{(Z)})^2+(g_{Ae}^{(Z)})^2][(\overline{g}_{Ve}^{(Z)})^2+(\overline{g}_{Ae}^{(Z)})^2]+4g_{Ve}^{(Z)}g_{Ae}^{(Z)}\overline{g}_{Ve}^{(Z)}\overline{g}_{Ae}^{(Z)})+\frac{u^2}{t^2}(\overline{g}_{Ve}^{(\gamma)})^4$$
$$\left.+\frac{2u^2}{t(t-M_Z^2)}(\overline{g}_{Ve}^{(\gamma)})^2[(\overline{g}_{Ve}^{(Z)})^2+(\overline{g}_{Ae}^{(Z)})^2]+\frac{u^2}{(t-M_Z^2)^2}\{[(\overline{g}_{Ve}^{(Z)})^2+(\overline{g}_{Ae}^{(Z)})^2]^2+4(\overline{g}_{Ve}^{(Z)}\overline{g}_{Ae}^{(Z)})^2\}\right\}, \tag{A2}$$

$$\frac{d\sigma^2}{d\cos\theta}=\frac{1}{16\pi q^2}\left\{\frac{q^4}{t^2}(\overline{g}_{Ve}^{(\gamma)})^4+\frac{2q^4}{t(t-M_Z^2)}(\overline{g}_{Ve}^{(\gamma)})^2[(g_{Ve}^{(Z)})^2-(g_{Ae}^{(Z)})^2]+\frac{q^4}{(t-M_Z^2)^2}\{[(\overline{g}_{Ve}^{(Z)})^2-(\overline{g}_{Ae}^{(Z)})^2]^2\}\right\}, \tag{A3}$$

TABLE VI. Linear collider. 95% C.L. bounds on nonuniversal new physics scales for the considered contact interactions and extra dimension models. Data sets and column meanings are as in Table V. Units are in TeV.

	Without Bhabha	With all Bhabha	σ	A_{LR}	$A_{\|\|}$	forw.	back.
Λ_{LL}	85	94	89	89	87	93	85
Λ_{RR}	84	92	87	88	85	92	84
Λ_{LR}	66	120	120	66	87	110	110
Λ_{RL}	81	130	120	81	94	110	110
Λ_{VV}	120	150	150	120	120	150	140
Λ_{AA}	110	140	130	110	120	120	130
Λ_{AV}	130	130	130	130	130	130	130
Λ_{VA}	71	90	71	90	71	90	71
Λ_{ED}	3.3	5.7	5.7	3.3	3.6	5.6	4.5

$$\frac{d\sigma^P}{d\cos\theta}=\frac{u^2}{4\pi q^2}\left\{\frac{1}{[(q^2-M_Z^2)^2+M_Z^2\Gamma_Z^2]}\left(\frac{q^2-M_Z^2}{q^2}(g_{Ve}^{(\gamma)})^2(g_{Ve}^{(Z)}g_{Ae}^{(Z)})+(g_{Ve}^{(Z)}g_{Ae}^{(Z)})[(g_{Ve}^{(Z)})^2+(g_{Ae}^{(Z)})^2]\right)\right.$$
$$+\frac{1}{q^2(t-M_Z^2)}(g_{Ve}^{(\gamma)})^2(\overline{g}_{Ve}^{(Z)}\overline{g}_{Ae}^{(Z)})+\frac{q^2-M_Z^2}{t[(q^2-M_Z^2)^2+M_Z^2\Gamma_Z^2]}(\overline{g}_{Ve}^{(\gamma)})^2(g_{Ve}^{(Z)}g_{Ae}^{(Z)})+\frac{q^2-M_Z^2}{(t-M_Z^2)[(q^2-M_Z^2)^2+M_Z^2\Gamma_Z^2]}$$
$$\times\{(g_{Ve}^{(Z)}g_{Ae}^{(Z)})[(\overline{g}_{Ve}^{(Z)})^2+(\overline{g}_{Ae}^{(Z)})^2]+(\overline{g}_{Ve}^{(Z)}\overline{g}_{Ae}^{(Z)})[(g_{Ve}^{(Z)})^2+(g_{Ae}^{(Z)})^2]\}$$
$$\left.+\frac{1}{t(t-M_Z^2)}(\overline{g}_{Ve}^{(\gamma)})^2(\overline{g}_{Ve}^{(Z)}\overline{g}_{Ae}^{(Z)})+\frac{1}{(t-M_Z^2)^2}\{\overline{g}_{Ve}^{(Z)}\overline{g}_{Ae}^{(Z)}[(\overline{g}_{Ve}^{(Z)})^2+(\overline{g}_{Ae}^{(Z)})^2]\}\right\}. \quad \text{(A4)}$$

[1] LEP Collaborations ALEPH, DELPHI, L3, Opal, the LEP Electroweak Working Group and the SLD Heavy Flavour and Electroweak Groups, CERN-EP/99-15.

[2] F. M. Renard and C. Verzegnassi, Phys. Rev. D **52**, 1369 (1995); **53**, 1290 (1996).

[3] F. M. Renard and C. Verzegnassi, Phys. Rev. D **55**, 4370 (1997); M. Beccaria, G. Montagna, O. Nicrosini, F. Piccinini, F. M. Renard, and C. Verzegnassi, *ibid.* **58**, 093014 (1998); M. Beccaria, P. Ciafaloni, D. Comelli, F. Renard, and C. Verzegnassi, Eur. Phys. J. C **10**, 331 (1999).

[4] A. Blondel, F. M. Renard, L. Trentadue, and C. Verzegnassi, Phys. Rev. D **54**, 5567 (1996); M. Beccaria, F. M. Renard, S. Spagnolo, and C. Verzegnassi, Phys. Lett. B **448**, 129 (1999).

[5] R. S. Chivukula, F. M. Renard, and C. Verzegnassi, Phys. Rev. D **57**, 2760 (1998).

[6] M. Beccaria, F. M. Renard, S. Spagnolo, and C. Verzegnassi, Phys. Lett. B **475**, 157 (2000).

[7] M. E. Peskin and T. Takeuchi, Phys. Rev. Lett. **65**, 964 (1990).

[8] G. Altarelli and R. Barbieri, Phys. Lett. B **253**, 161 (1991).

[9] M. Beccaria, P. Ciafaloni, D. Comelli, F. M. Renard, and C. Verzegnassi, Phys. Rev. D **61**, 073005 (2000).

[10] K. Hagiwara, S. Ishihara, R. Szalapski, and D. Zeppenfeld, Phys. Rev. D **48**, 2182 (1993).

[11] E. Eichten, K. Lane, and M. Peskin, Phys. Rev. Lett. **50**, 811 (1983).

[12] B. Schrempp, F. Schrempp, N. Wermes, and D. Zeppenfeld, Nucl. Phys. **B296**, 1 (1988).

[13] J. Hewett, Phys. Rev. Lett. **82**, 4765 (1999); T. Rizzo, Phys. Rev. D **59**, 115010 (1999).

[14] LEP EWWG $f\bar{f}$ Subgroup, ''Combination of the LEP2 $f\bar{f}$ Results,'' LEP2FF/99-01, ALEPH 99-082 PHYSIC 99-030, DELPHI 99-143 PHYS 829, L3 Note 2443, OPAL TN616; LEP EWWG $f\bar{f}$ Subgroup: http://www.cern.ch/LEPEWWG/lep2/.

[15] The OPAL Collaboration, G. Abbiendi *et al.*, ''Test of the Standard Model and Constraints on New Physics from Measurements of Fermion Pair Production at 189 GeV at LEP,'' CERN-EP/99-097, 1999.

[16] ZFITTER, D. Bardin *et al.*, Phys. Lett. B **255**, 290 (1991); Nucl. Phys. **B351**, 1 (1991); Z. Phys. C **44**, 493 (1989).

[17] TOPAZ0, G. Montagna, O. Nicrosini, G. Passarino, F. Piccinini, and R. Pittau, Comput. Phys. Commun. **76**, 328 (1993).

[18] KK2f, S. Jadach, B. F. L. Ward, and Z. Wąs, Phys. Lett. B **449**, 97 (1999).

[19] BHWIDE, S. Jadach, W. Placzek, and B. F. L. Ward, Phys. Lett. B **390**, 298 (1997).

[20] ALIBABA, W. Beenakker *et al.*, Nucl. Phys. **B349**, 323 (1991).

[21] F. M. Renard and C. Verzegnassi, Phys. Rev. D **55**, 4370 (1997); M. Beccaria, F. M. Renard, S. Spagnolo, and C. Verzegnassi, ''New Physics Effects from $e^+e^-\to\bar{f}f$ at a Linear Collider: the role of $A_{LR,\mu}$, DESY/ECFA Report No. LC-TH-1999-016.

[22] D. Bourilkov, J. High Energy Phys. **08**, 006 (1999).